EDGE ARTICLE

Check for updates

All publication charges for this article have been paid for by the Royal Society of Chemistry

Nickel boryl complexes and nickel-catalyzed alkyne borylation†

Lukas Tendera,‡[a] Felipe Fantuzzi, [ID] ‡[b] Todd B. Marder [ID] [ac] and Udo Radius [ID] *[a]

The first nickel bis-boryl complexes *cis*-[Ni(^{i}Pr$_2$Im^{Me})$_2$(Bcat)$_2$], *cis*-[Ni(^{i}Pr$_2$Im^{Me})$_2$(Bpin)$_2$] and *cis*-[Ni(^{i}Pr$_2$Im^{Me})$_2$(Beg)$_2$] are reported, which were prepared *via* the reaction of a source of [Ni(^{i}Pr$_2$Im^{Me})$_2$] with the diboron(4) compounds B$_2$cat$_2$, B$_2$pin$_2$ and B$_2$eg$_2$ (^{i}Pr$_2$Im^{Me} = 1,3-di-iso-propyl-4,5-dimethylimidazolin-2-ylidene; B$_2$cat$_2$ = bis(catecholato)diboron; B$_2$pin$_2$ = bis(pinacolato)diboron; B$_2$eg$_2$ = bis(ethylene glycolato)diboron). X-ray diffraction and DFT calculations strongly suggest that a delocalized, multicenter bonding scheme dictates the bonding situation of the NiB$_2$ moiety in these square planar complexes, reminiscent of the bonding situation of "non-classical" H$_2$ complexes. [Ni(^{i}Pr$_2$Im^{Me})$_2$] also efficiently catalyzes the diboration of alkynes using B$_2$cat$_2$ as the boron source under mild conditions. In contrast to the known platinum-catalyzed diboration, the nickel system follows a different mechanistic pathway, which not only provides the 1,2-borylation product in excellent yields, but also provides an efficient approach to other products such as C−C coupled borylation products or rare tetra-borylated compounds. The mechanism of the nickel-catalyzed alkyne borylation was examined by means of stoichiometric reactions and DFT calculations. Oxidative addition of the diboron reagent to nickel is not dominant; the first steps of the catalytic cycle are coordination of the alkyne to [Ni(^{i}Pr$_2$Im^{Me})$_2$] and subsequent borylation at the coordinated and, thus, activated alkyne to yield complexes of the type [Ni(NHC)$_2$(η^2-*cis*-(Bcat)(R)C=C(R)(Bcat))], exemplified by the isolation and structural characterization of [Ni(^{i}Pr$_2$Im^{Me})$_2$(η^2-*cis*-(Bcat)(Me)C=C(Me)(Bcat))] and [Ni(^{i}Pr$_2$Im^{Me})$_2$(η^2-*cis*-(Bcat)(H$_7$C$_3$)C=C(C$_3$H$_7$)(Bcat))].

Introduction

Numerous homogeneous catalytic borylation reactions have been developed over the past decades,[1] which include the Suzuki–Miyaura borylation of aryl and alkyl halides,[2] catalytic addition reactions to unsaturated organic molecules such as alkenes, alkynes, allenes, α,β-unsaturated compounds, and carbonyl compounds *via* hydroboration, diboration, β-borylation or carboboration,[3,4] or the direct functionalization of C–H bonds.[5] In all of these transformations, transition metal boryl complexes[6] play a pivotal role and are key intermediates.[7] Thus, research on transition metal boryl complexes [L$_n$M-BX$_2$], in general, is attractive due to their interesting properties and

their utility in catalysis, in which poly-boryl complexes often play a dominant role. Among the most important transition metal poly-boryl complexes employed in catalysis are iridium tris-boryl or rhodium bis-boryl complexes, initially synthesized by Marder and Baker *et al.* in 1993 (Fig. 1: compounds **I** and **III**),[8] and nowadays frequently employed for C–H borylations of arenes, alkenes, and alkanes.[5,9,10] Complexes such as [Ir(dtbpy)(COE)(Bpin)$_3$] **II** (Fig. 1, dtbpy = di-*tert*-butylbipyridine, COE = cyclooctene; pin = pinacolato)[9a] are key catalytic intermediates in iridium-catalyzed C–H borylation reactions.
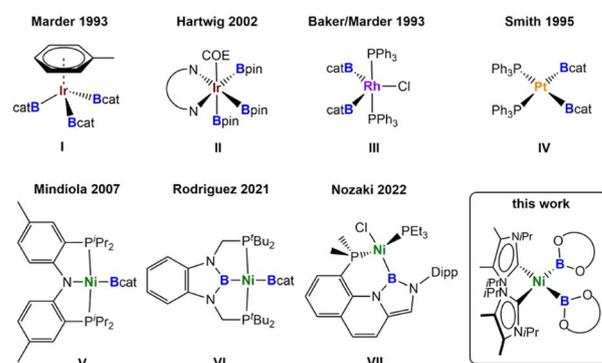
[a]Institute for Inorganic Chemistry, Julius-Maximilians-Universität Würzburg, Am Hubland, 97074 Würzburg, Germany. E-mail: u.radius@uni-wuerzburg.de

[b]School of Chemistry and Forensic Science, University of Kent, Park Wood Rd, Canterbury, CT2 7NH, UK

[c]Institute for Sustainable Chemistry & Catalysis with Boron, Julius-Maximilians-Universität Würzburg, Am Hubland, 97074 Würzburg, Germany

† Electronic supplementary information (ESI) available: Additional figures, experimental section, crystallographic details, NMR spectra, computational details. CCDC 2202537–2202552. For ESI and crystallographic data in CIF or other electronic format see DOI: https://doi.org/10.1039/d2sc04690c

‡ These authors contributed equally.

Fig. 1 Selected examples of transition-metal boryl complexes.

Another well studied class of poly-boryl complexes are platinum bis-boryl complexes such as *cis*-[Pt(PPh$_3$)$_2$(Bcat)$_2$] **IV** (cat = catecholato),[11] pre-catalysts for the addition of diborane(4) compounds to alkynes, reported independently by the groups of Suzuki and Miyaura,[12a,b] Smith III,[12c] and Marder and Norman.[13] The platinum-catalyzed insertion of alkynes into the B–B bond of a diborane(4) reagent is of interest as it provides the most atom economical route for the stereoselective synthesis of tri- and tetra-substituted alkenes.[4] The resulting 1,2-diboryl alkenes are important building blocks in organic synthesis and materials science.[14]

Most of the transition metal-catalyzed borylation reactions developed initially employed precious metals as the catalyst precursors. As first-row d-block metals are less toxic, less expensive, Earth-abundant, and environmentally benign, they are very attractive alternatives to these expensive noble metals. Recently developed borylations employing 3d-metal catalysts show excellent reactivity and selectivity and often facilitate unique transformations previously unobserved in traditional precious metal-catalyzed processes.[1h] Good examples for outstanding reactivity are copper(I) boryl complexes, using a diverse range of ligands with phosphines and NHCs (N-heterocyclic carbenes) being the most commonly employed. These reagents are attractive for different transformations, featuring mild reaction conditions, good functional group tolerance, and low cost of the metal catalyst.[1h,15] For example, *in situ* generated copper boryl complexes of the type [LCu(Bpin)] (L = phosphine or NHC) have been employed successfully in the borylation of aryl or alkyl chlorides, bromides, and iodides.[15]

We recently investigated the use of NHC nickel complexes for the borylation of aryl chlorides, aryl fluorides, and indoles.[16] For each of our nickel-catalyzed borylation reactions, a nickel boryl complex was proposed as a key intermediate, but has never been fully characterized *in situ* or isolated.[17] Nickel boryl complexes are generally considered to be elusive, in contrast to other 3d-metals such as iron,[18] cobalt,[19] or copper.[15,20] Only a few structurally characterized nickel boryl complexes have been isolated thus far, all of them bearing large, rigid pincer ligands (Fig. 1). In 2007, Mindiola *et al.*[21a,b] reported the synthesis of the first nickel mono-boryl complex [(PNP)Ni(Bcat)] **V** (PNP = N[2-P(CHMe$_2$)$_2$-4-methylphenyl]$_2$). In 2014, Peters *et al.*[21c] and Rodriguez *et al.*[21d] independently reported several boryl complexes of PBP pincer ligands [(^{tBu}PBP)NiL] (L = H, Cl, Br, OTf, OC(H)O, Me; ^{tBu}PBP = C$_6$H$_4${N(CH$_2$P^{t}Bu$_2$)}$_2$B), in which the boryl moiety is embedded in the pincer system. They also introduced a dimeric nickel(I) complex [(^{Ph}PBP)Ni]$_2$ with bridging boryl ligands (^{Ph}PBP = C$_6$H$_4${N(CH$_2$PPh$_2$)}$_2$B) and the first bis-boryl complex [(^{tBu}PBP)Ni(Bcat)] **VI**.[21c,e] Very recently, Nozaki *et al.* reported the phosphine/boryl chelating complex **VII** (Fig. 1), synthesized *via* dehydrochloroborylation of a nickel(0) σ-borane precursor.[21f]

Results and discussion

Synthesis and characterization of nickel boryl complexes

We recently investigated, in detail, the differences in the reactivity of NHC nickel complexes of the type [Ni(NHC)$_2$]

dependent upon the stereo-electronic features of the NHC ligands,[22] which was the key to the success of the present study. In earlier work, we found that reactions of synthetic equivalents of the complexes [Ni(^{i}Pr$_2$Im)$_2$], [Ni(Cy$_2$Im)$_2$], and [Ni(Mes$_2$Im)$_2$] (R$_2$Im = 1,3-di-organyl-imidazolin-2-ylidene; Cy = cyclohexyl; Mes = mesityl; ^{i}Pr = iso-propyl) with B$_2$cat$_2$, B$_2$pin$_2$, or B$_2$eg$_2$ (=bis(ethylene glycolato)diboron) did not lead to isolable nickel boryl complexes. For the smaller NHCs, decomposition with formation of nickel black and NHC diborane adducts typically occurred. The NHC diborane adducts often underwent subsequent NHC ring expansion reactions, which destroyed the core structure of the NHC and made the process irreversible.[23] Furthermore, in the course of our work on the defluoroborylation of polyfluoroarenes, on the borylation of aryl chlorides, and on the C–H borylation of indoles using [Ni(Mes$_2$Im)$_2$] as a catalyst,[16] we postulated nickel boryl complexes as decisive intermediates, but never detected such compounds. Complexes of the type [Ni(Mes$_2$Im)$_2$(Ar^F)(B{OR}$_2$)] (B{OR}$_2$ = Bcat, Bpin) were not observed in stoichiometric reactions of [Ni(Mes$_2$-Im)$_2$(Ar^F)F] with B$_2$pin$_2$ or B$_2$cat$_2$, as reductive elimination leading to the borylation product Ar^F-B(OR)$_2$ was rapid, reforming [Ni(Mes$_2$Im)$_2$].[16a] However, in the course of our work on the borylation of aryl chlorides, a resonance at 44.5 ppm was observed in the ^{11}B{^{1}H} NMR spectrum for the reaction of [Ni(Cy$_2$Im)$_2$(Ar)Cl] with B$_2$pin$_2$, which indicated the formation of a nickel boryl complex.[16d] Unfortunately, this complex of the *N*-cyclohexyl-substituted NHC was not stable in solution and defied isolation despite several attempts. Therefore, we reasoned that using an NHC ligand with similar donor properties and only slightly modified steric demand might lead to the successful synthesis of nickel boryl complexes. As it has been demonstrated previously that backbone substitution at the C4 and C5 position of the imidazole framework by methylation effects the sterics of the NHC ligands as repulsion between the C4/C5 methyl group and the *N*-organyl substituent leads to smaller C$_{carbene}$-*N*-C$_{substituent}$ angles,[24] we used synthetic equivalents of the backbone-methylated [Ni(^{i}Pr$_2$Im^{Me})$_2$] for this study.

[Ni(^{i}Pr$_2$Im^{Me})$_2$] was provided from a mixture of [Ni$_2$(^{i}Pr$_2$-Im^{Me})$_4$(µ-(η^2:η^2)-COD)] **1** and [Ni(^{i}Pr$_2$Im^{Me})$_2$(η^4-COD)] **1a**, which can be prepared by the reaction of [Ni(COD)$_2$] with two equivalents of ^{i}Pr$_2$Im^{Me}, as reported previously.[22l] The stoichiometric
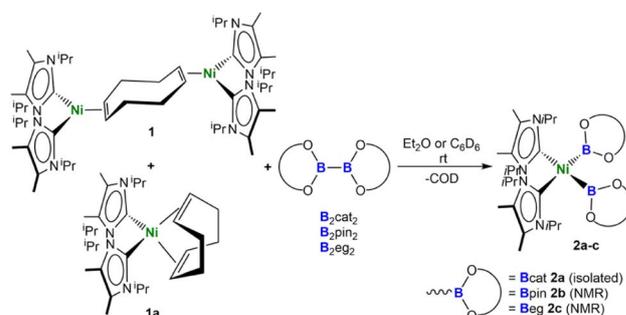
Scheme 1 Synthesis of *cis*-[Ni(^{i}Pr$_2$Im^{Me})$_2$(Bcat)$_2$] **2a**, *cis*-[Ni(^{i}Pr$_2$Im^{Me})$_2$(Bpin)$_2$] **2b**, and *cis*-[Ni(^{i}Pr$_2$Im^{Me})$_2$(Beg)$_2$] **2c**.

reaction of such a mixture of **1** and **1a** with B$_2$cat$_2$ at room temperature cleanly led to the formation of cis-[Ni(^{i}Pr$_2$Im^{Me})$_2$(-Bcat)$_2$] **2a** (Scheme 1), which is the first cis-nickel bis-boryl complex synthesized and isolated thus far. This complex was isolated as a pale brown solid in 58% yield and was characterized by IR- and NMR-spectroscopy, X-ray diffraction, and elemental analysis (vide infra).

If the reaction was carried out with either B$_2$pin$_2$ or B$_2$eg$_2$ instead of B$_2$cat$_2$, it did not proceed quantitatively at room temperature, even if a large excess of the diboron(4) reagent was employed. In all cases, the reaction started at approximately 0 °C, but did not proceed at lower temperatures. An increase of the temperature above room temperature rapidly led to a darkening of the reaction mixture with decomposition of the bis-boryl complexes, which is especially rapid for **2b** and **2c**. This behavior reflects that of copper(I) boryl complexes, which easily decompose upon warming.[20d–g] The use of modified starting materials, such as the ethylene complex [Ni(^{i}Pr$_2$Im^{Me})$_2$(η^2-C$_2$H$_4$)] **1b** or the cyclooctene (COE) complex [Ni(^{i}Pr$_2$Im^{Me})$_2$(η^2-COE)] **1c** (see ESI†), was also unsuccessful for the bulk production of pure **2b** and **2c**. However, the formation of the bis-boryl complexes cis-[Ni(^{i}Pr$_2$Im^{Me})$_2$(Bpin)$_2$] **2b** and cis-[Ni(^{i}Pr$_2$Im^{Me})$_2$(Beg)$_2$] **2c** was clearly detected by NMR spectroscopy, and small amounts of these complexes suitable for X-ray diffraction crystallized from these reaction mixtures (Fig. 2). The bis-boryl complexes reveal different stabilities in solution. Whereas cis-[Ni(^{i}Pr$_2$Im^{Me})$_2$(Bpin)$_2$] **2b** was still detected in the reaction mixture in a solution kept at room temperature for one month, complexes **2a** and **2c** completely decompose in C$_6$D$_6$ over a period of 6–14 days with formation of multiple, as yet unidentified, species.

Characteristic for complexes **2a–c** is a broad resonance at 48.7 ppm (**2a**), 46.1 ppm (**2b**), and 46.5 ppm (**2c**) in the ^{11}B{^{1}H} NMR spectrum (see Table 1), which is the region typically observed for transition metal boryl complexes,[6] c.f. 47.0 ppm for cis-[Pt(PPh$_3$)$_2$(Bcat)$_2$].[13] In the ^{13}C{^{1}H} NMR spectra, the NHC carbene carbon resonances are also significantly shifted compared to those of the starting materials **1** (206.5 ppm) and **1a** (205.4 ppm) to 194.3 ppm (**2a**), 199.4 ppm (**2b**), and 198.5 ppm (**2c**). The complexes adopt cis-configurations in solution as their ^{1}H NMR spectra indicate pseudo-C_{2v} species with two resonances for the N-iso-propyl methyl protons (**2a**: 1.28 ppm and 1.45 ppm, **2b**: 1.32 ppm and 1.69 ppm, **2c**: 1.28 ppm and 1.58 ppm) and only one signal for the N-iso-propyl methine (**2a**: 6.05 ppm, **2b**: 5.99 ppm, **2c**: 6.04 ppm) and for the backbone methyl protons (**2a**: 1.63 ppm, **2b**: 1.84 ppm, **2c**: 1.78 ppm).

Crystals suitable for X-ray diffraction of **2a–c** were obtained by storing the reaction mixtures in diethylether at −30 °C. Complexes **2a–c** crystallize in the triclinic space group P$\bar{1}$ and adopt a distorted square planar geometry with cis-boryl ligands, as observed for platinum bis-boryl complexes cis-[Pt(PR$_3$)$_2$(B{OR}$_2$)$_2$].[6,11] The Ni–C and Ni–B distances lie in a narrow range between 1.9092(18) Å and 1.9448(15) Å (see Table 1). We attribute the formation of cis-configured complexes to the strong trans-influence of the boryl ligands[25] and a remaining B–B interaction between the two boryl boron atoms (vide infra). This situation is similar to that observed previously for NHC-stabilized bis-silyl and hydro–silyl complexes cis-[Ni(NHC)$_2$(-SiR$_3$)$_2$] and cis-[Ni(NHC)$_2$(H)(SiR$_3$)].[26] The B–B separations of 2.156(3) Å (**2a**), 2.247(3) Å (**2b**), and 2.189(4) Å (**2c**) (see Table 1)
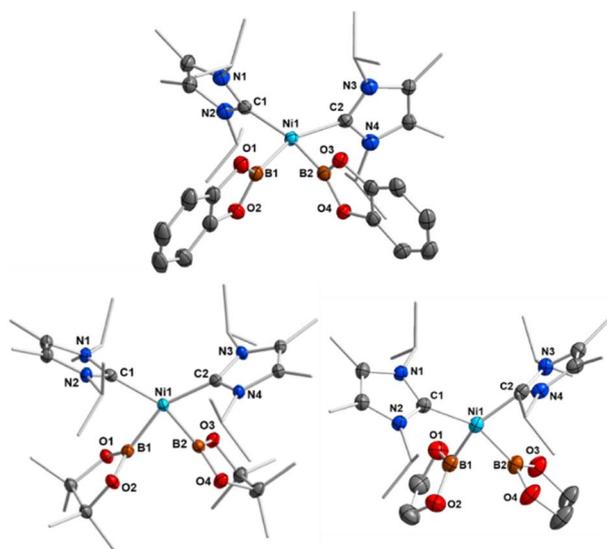

Fig. 2 Molecular structures of cis-[Ni(^{i}Pr$_2$Im^{Me})$_2$(Bcat)$_2$] **2a** (top), cis-[Ni(^{i}Pr$_2$Im^{Me})$_2$(Bpin)$_2$] **2b** (bottom left), and cis-[Ni(^{i}Pr$_2$Im^{Me})$_2$(Beg)$_2$] **2c** (bottom right) in the solid state (ellipsoids shown at 50% probability level). Hydrogen atoms are omitted for clarity. For selected bond lengths and angles see Table 1 and ESI Fig. S4–S6.†

Table 1 Important bond lengths, bond angles and chemical shifts of cis-[Ni(^{i}Pr$_2$Im^{Me})$_2$(Bcat)$_2$] **2a**, cis-[Ni(^{i}Pr$_2$Im^{Me})$_2$(Bpin)$_2$] **2b**, cis-[Ni(^{i}Pr$_2$-Im^{Me})$_2$(Beg)$_2$] **2c**, and [(PNP)Ni(Bcat)] **V** (δ_B B(OR)$_2$ = ^{11}B{^{1}H} NMR shift of the boron atoms, δ_c NHC = ^{13}C{^{1}H} NMR shift of the NHC carbene carbon atoms)

|	Ni–B (Å)	B–B (Å)	Ni–C (Å)	B–Ni–B (°)	δ_B B(OR)$_2$ (ppm)	δ_c NHC [ppm]
2a	1.9231(19)	2.156(3)	1.9393(16)	68.45(7)	48.7	194.3
	1.9092(18)		1.9448(15)			
2b	1.936(2)	2.247(3)	1.9318(18)	70.82(8)	46.1	199.4
	1.942(2)		1.9185(17)			
2c	1.939(2)	2.189(4)	1.9180(15)	68.79(8)	46.5	198.5
	1.9353(19)		1.9265(17)			
V[21a]	1.9091(18)	—	—	—	47.0	—

are much smaller than those observed for bis-boryl platinum complexes (2.451–2.667 Å),[11–13] consistent with small B1–Ni–B2 angles of 68.45(7)° (**2a**), 70.82(8)° (**2b**), and 68.79(8)° (**2c**).

Thus, the B–B distances are only 0.478 Å (**2a**), 0.540 Å (**2b**), and 0.485 Å (**2c**) longer than those in the solid state molecular structures of B_2cat_2 (1.678(3) Å), B_2pin_2 (1.707(5) Å), and B_2eg_2 (1.704(3) Å).[23d,27] The BO_2 planes of both boryl ligands are nearly perpendicular to the NiC_2B_2 square plane with angles of 87.85(7)° and 86.21(6)° (**2a**), 88.41(9)° and 88.07(9)° (**2b**), and 85.85(10)° and 85.30(10)° (**2c**). Thus, the structures are best represented by valence tautomer **B** in Scheme 2, which lies in-between the limiting structures of a Ni(ii) bis-boryl complex **A** and a Ni(0) diborane(4) complex **C**, i.e., incomplete oxidative addition with a residual B⋯B interaction. This is reminiscent of "non-classical" H_2 complexes. As the Ni–B distances of 1.9231(19) Å and 1.9092(18) Å (**2a**), 1.936(2) Å and 1.942(2) Å (**2b**), and 1.939(2) Å and 1.9353(19) Å are of similar magnitude as those observed in [(PNP)Ni(Bcat)] **V** (1.9091(18) Å)[21a] and [(PBP)Ni(Bcat)] **VI** (1.942(2) Å; 2.015(2) Å),[21d] which feature 2-center-2-electron Ni–B bonds, the oxidative addition is nearly complete.

This situation is closely related to that observed for the paramagnetic cobalt complexes [Co(PMe₃)₃(Bcat)₂] (B–B: 2.185 Å, B–Co–B: 67.9(4)°) and mer-[Co(PMe₃)₃(Bcat)₃] (B–B: 2.1541(5) Å, B–Co–B: 65.78(1) °), which also feature two Bcat ligands with short B–B distances.[19a,g] DFT calculations on mer-[Co(PMe₃)₃(Bcat)₃] revealed bond critical points at the Co–B vector with substantial electron densities and a bond critical point along the B–B vector, which was characterized by a substantial electron density associated with a much smaller yet positive Laplacian compared to the Co–B bond. It was concluded that mer-[Co(PMe₃)₃(Bcat)₃] maintains a degree of B–B interaction, which is essential for the stabilization of this boryl complex.

The preference for isomer **B** to describe the bonding situation of the NiB_2 motif in **2a–c** is also supported by DFT computations on complex **2a**. Inspection of the canonical Kohn–Sham molecular orbitals of **2a** reveals that the HOMO (Fig. 3a) is mainly composed of a combination of 3d orbitals of nickel that expands across the B–B bonding region. Accordingly, a Mayer bond order (MBO)[28] of 0.451 is found for the B–B bond, whereas the corresponding MBOs of the Ni–B bonds are 0.711 each. These findings strongly suggest that a delocalized, multicenter bonding scheme dictates the bonding situation of the NiB_2 moiety. This picture is corroborated by further calculations based on the intrinsic bond orbital (IBO) approach.[29]
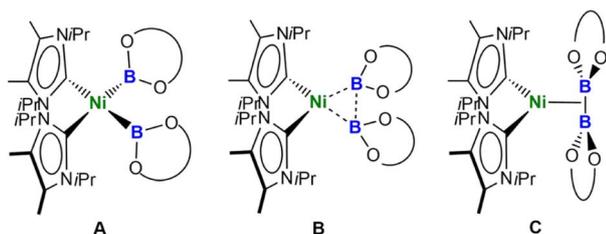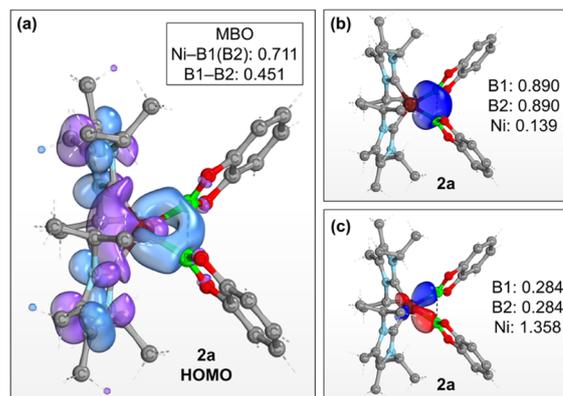

Fig. 3 (a) HOMO of **2a** (isovalue: 0.03 au). The Ni–B and B–B Mayer bond orders of **2a** are shown in the top right box. (b) and (c) Intrinsic bond orbitals of **2a** involved in the bonding of the NiB_2 motif. Numerical values indicate the fraction of electrons of the doubly occupied orbital assigned to the individual atoms. Level of theory: PBE0-D3(BJ)/def2-SVP/def2-TZVP(Ni).[30] Hydrogen atoms are omitted for clarity.

Analysis of the IBOs of **2a** indicates that two doubly occupied IBOs are participating in the NiB_2 bonding. The first orbital (Fig. 3b) is mainly localized at the B–B bonding region, with partial delocalization on the Ni center and across the Ni–B bonds. In contrast, the second orbital (Fig. 3c) is mostly localized across the Ni–B bonds, but with a larger contribution coming from the Ni center. From the IBO point of view, the bonding situation of the NiB_2 motif is better described as composed of two three-center two-electron (3c,2e) bonds. Taken together, these results are in accordance with the analysis based on the X-ray structures of **2a–c** and support the multicenter bonding situation depicted in isomer **B**.

Nickel-catalyzed borylation of alkynes

Bis-boryl complexes are regarded as the key intermediates for the catalytic diboration of alkynes in platinum chemistry.[11–13] It has been demonstrated that complexes cis-[Pt(PR₃)₂(Bcat)₂] or synthetic equivalents for [Pt(PR₃)₂] are highly active catalyst precursors for the cis-stereospecific diboration of alkynes and 1,3-diynes. In the platinum system, phosphine dissociation is a critical step in the catalytic cycle (see ESI Fig. S1†), which includes formation of the bis-boryl complex cis-[Pt(PR₃)₂(B{OR}₂)₂] from the catalyst precursor and subsequent phosphine dissociation to give sterically and electronically unsaturated [Pt(PR₃)(B{OR}₂)₂]. This complex can add the alkyne, and insertion of the alkyne into the Pt–B{OR}₂ bond and reductive elimination lead to the corresponding cis-alkene-1,2-bis(boronate) ester with regeneration of [Pt(PR₃)] or [Pt(PR₃)₂]. DFT calculations have shown that similar Pd(0) complexes cannot catalyze the alkyne diboration due to differences in the oxidative addition step of the B–B bond of the diborane to [M(PR₃)₂].[12d] Although the kinetic barrier is lower, the addition is endothermic for the palladium complex and thus the addition product is not stable due to a very small reverse barrier. For the diboration of alkynes using B_2pin_2 as the boron source, the

Scheme 2 Valence tautomers of complexes cis-[Ni(^{i}Pr₂Im^{Me})₂(B{OR}₂)₂] **2a–c**.

optimized phosphine:platinum ratio was later shown to be 1 : 1, with catalyst activity being strongly dependent on the nature of the phosphine.[13b] Sterically bulky, strong electron donors, such as PCy$_3$, allowed diborations to be performed at ambient temperatures. Thus, the isolable and stable compound [Pt(PCy$_3$)(η^2-C$_2$H$_4$)$_2$] was shown to be an excellent catalyst precursor for alkyne diboration even at room temperature.[13b] We were thus interested to see whether our nickel complexes are also able to catalyze this reaction.

Catalytic reactions were typically carried out in Youngs tap-NMR tubes using different internal and terminal alkynes (see Table 2). As standard reaction conditions, 4 mol% of [Ni(^{i}Pr$_2$-Im^{Me})$_2$] (the mixture of **1** and **1a** was used directly) and equimolar amounts of alkyne and B$_2$cat$_2$ were reacted using C$_6$D$_6$ as the solvent at 50 °C. Reaction progress was monitored via ^{1}H and ^{11}B{^{1}H} NMR spectroscopy. After completion, the resulting products were identified by NMR spectroscopy and GC/MS analysis of the reaction mixture. Internal alkynes led selectively to the quantitative formation of the cis-1,2-diborylalkenes Z-(Bcat)(Ph)C=C(Ph)(Bcat) **3**, Z-(Bcat)(4-Me-C$_6$H$_4$)C=C(4-Me-C$_6$H$_4$)(Bcat) **4**, Z-(Bcat)(4-CF$_3$-C$_6$H$_4$)C=C(4-CF$_3$-C$_6$H$_4$)(Bcat) **5**, Z-(Bcat)(C$_3$H$_7$)C=C(C$_3$H$_7$)(Bcat) **6**, and Z-(Bcat)(Me)C=C(Ph)(Bcat) **7**. However, for the synthesis of **3**, **4**, and **5**, a higher catalyst loading of 10 mol% was necessary to reach full conversion as the catalyst is deactivated by transfer of the NHC ligands to the borylation product to yield the corresponding mono NHC-adducts (vide infra). The NHC adduct of compound **4**, Z-(Bcat)(4-Me-C$_6$H$_4$)C=C(4-Me-C$_6$H$_4$)(Bcat)·(^{i}Pr$_2$Im^{Me}) **4^{NHC}**, was isolated and characterized separately by the reaction of **4** with one equivalent of ^{i}Pr$_2$Im^{Me} (see Scheme 3).

The reaction of aryl substituted terminal alkynes also led to the formation of the cis-1,2-diborylalkenes E-(Bcat)HC=C(Ph)(Bcat) **9**, E-(Bcat)HC=C(4-Me-C$_6$H$_4$)(Bcat) **10** and E-(Bcat)HC=C(4-^{t}Bu-C$_6$H$_4$)(Bcat) **11**, but after consumption of the alkyne, approximately 40% unreacted B$_2$cat$_2$ was always detected besides the 1,2-diborylalkene products. Analysis of the reaction mixtures via high resolution mass spectrometry revealed that alkyne cyclotrimerization products and different partially borylated coupling products were formed as side-products, which are hard to identify via NMR spectroscopy (see ESI, Fig. S72–S83†). Note that the use of more than one equivalent of the alkynes inhibits the borylation, so that no transformation at all was observed when 4 equivalents of the alkynes were used.

Compared to the well-established platinum catalysts,[12,13] our nickel complex shows very good activity towards internal alkynes under mild conditions. Only the mono-phosphine platinum complexes reported by Marder et al.[13b] show a higher efficiency, as they catalyze the diboration at room temperature with a low catalyst loading. For terminal alkynes, the platinum diphosphine complexes and, especially, the palladium NHC complex [Pd(Me$_2$Im^{Me})$_2$(η^2-PhC≡CPh)] reported by Navarro et al., deliver higher yields (79–95%).[31] Interestingly, the reactions of alkyl substituted 1-pentyne or TMS-substituted N,N-dimethyl-4-[(trimethylsilyl)-ethynyl] aniline led to new, previously unknown reaction products. The borylation of 1-pentyne selectively afforded the C–C coupled borylation products Z,Z-(Bcat)HC=C(C$_3$H$_7$)–(C$_3$H$_7$)C=

Table 2 Scope of the borylation of internal and terminal alkynes

^{a} Reaction conditions: [Ni(^{i}Pr$_2$Im^{Me})$_2$] **1/1a** (4 mol%), alkyne (1.0 equiv), B$_2$cat$_2$ (1.0 equiv), C$_6$D$_6$ (0.6 mL), 50 °C (if not otherwise stated). Products after total consumption of the alkynes, monitored by NMR and GC/MS. Yields are combined yields of the products and were estimated by ^{1}H-NMR with respect to the consumption of B$_2$cat$_2$. ^{b} [Ni(^{i}Pr$_2$Im^{Me})$_2$] **1/1a** (10 mol% needed for completion). ^{c} Excess of alkyne (>4 equiv). Products after total consumption of B$_2$cat$_2$. ^{d} B$_2$cat$_2$ (2 equiv).

CH(Bcat) **12a** (for proof of connectivity see ESI Fig. S18†) and E/Z,E/Z-(Bcat)HC=C(C$_3$H$_7$)–HC=C(Bcat)(C$_3$H$_7$) **12b** in a 3 : 2 ratio, according to NMR and GC/MS analysis. An excess of 1-pentyne (4 equiv.) was needed to reach full consumption of B$_2$cat$_2$. On the other hand, the borylation of the TMS-substituted alkyne selectively afforded the formation of polyborylated (4-NMe$_2$-C$_6$H$_4$)(Bcat)(TMS)C–C(Bcat)$_3$ **13**. In this
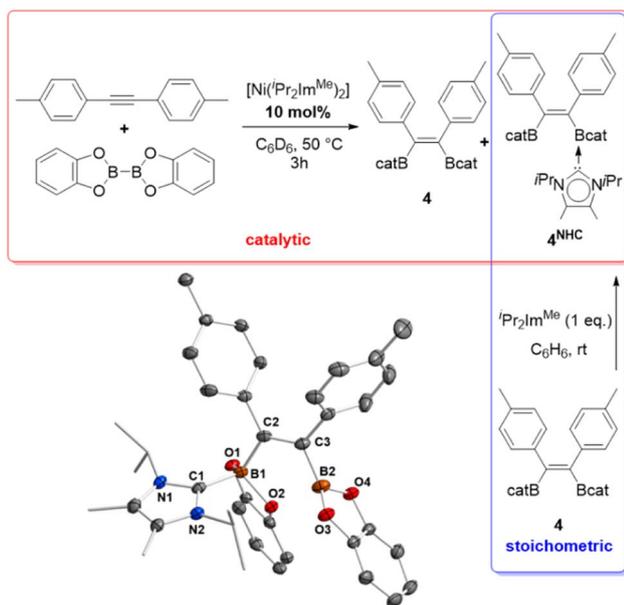
Scheme 3 Deactivation of the catalyst and independent synthesis of Z-(Bcat)(4-Me-C$_6$H$_4$)C=C(4-Me-C$_6$H$_4$)(Bcat)·(^{i}Pr$_2$Im^{Me}) **4^{NHC}**. For selected bond lengths and angles in **4^{NHC}** see Fig. S17 in the ESI.†

case, 2 equivalents of B$_2$cat$_2$ were needed for a full conversion and the TMS-group undergoes a formal 1,2-shift. Insertion of transition metal complexes into C(sp)–SiMe$_3$ bonds of alkynyl silanes were observed previously and are well explored in platinum chemistry.[13a,32] C(sp)–Si cleavage of Ar–C≡C–SiMe$_3$ should result in the formation of TMS–Bcat and Ar–C≡C–Bcat, which can react together in a transition metal-catalyzed reaction. The resulting product can then be diborated to yield different isomers Ar–C$_2$(Bcat)$_4$(SiMe$_3$), which have been observed for platinum-catalyzed reactions.[33] Therefore, the high yield synthesis of **13** is remarkable.

As we observed the formation of coupled and tetra-borylated products **12a/b** and **13**, we had a closer look at the catalytic borylation reaction of the internal alkyne 2-butyne, which is another special case (Scheme 4).

The reaction of 2-butyne with B$_2$cat$_2$ and [Ni(^{i}Pr$_2$Im^{Me})$_2$] as a catalyst afforded three different reaction products depending on the reaction conditions used, namely Z-(Bcat)(Me)C=C(Me)(Bcat) **8**, (Bcat)$_2$(Me)C–C(Me)(Bcat)$_2$ **8a** or E,E-(Bcat)(Me)
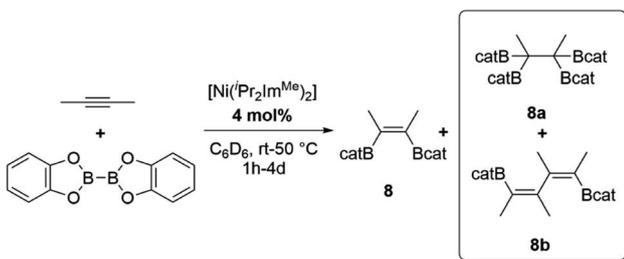
C=C(Me)–(Me)C=C(Me)(Bcat) **8b** (compare Scheme 4). The products obtained were often mixtures which cannot be separated by column chromatography, but the product ratios can be controlled to some extent via the ratio of alkyne to B$_2$cat$_2$ employed. The reaction of one equivalent of 2-butyne with a slight excess of B$_2$cat$_2$ and 4 mol% of [Ni(^{i}Pr$_2$Im^{Me})$_2$] (**1** and **1a**) in C$_6$D$_6$ was monitored by ^{1}H- and ^{11}B{^{1}H}-NMR spectroscopy, which showed complete consumption of the alkyne and B$_2$cat$_2$ after 3 h at 50 °C. NMR spectroscopy and GC/MS analysis of the final reaction products revealed the selective formation of the bis-borylated product Z-(Bcat)(Me)C=C(Me)(Bcat) **8** as the main product and traces of tetra-borylated product (Bcat)$_2$(Me)C–C(Me)(Bcat)$_2$ **8a** in a combined quantitative yield. If 2 equivalents of B$_2$cat$_2$ were used, **8a** was formed exclusively in quantitative yields. Applying a large excess of 2-butyne (>4 equiv.) led to a mixture of **8**, **8a** and **8b**, with **8b** being the main product, after full consumption of the diboron reagent (4d, rt). To our knowledge, the formation of compounds **8a** and **13** are the only examples for tetra-borylation of alkynes, beside the Pt-catalyzed tetra-borylation of (Bcat)C≡C(Bcat) to yield hexa-borylated ethane (Bcat)$_3$C–C(Bcat)$_3$, which was reported by Siebert et al. in 1999.[34] Products **8b** and **12a/b** are very rare examples for a combined one-step coupling and borylation of alkynes, which was first described by Marder et al., who observed small amounts of coupling products (via GC/MS) during the borylation of phenylacetylene with their platinum-catalyst.[13a] In recent years, Buñuel and Cárdenas et al. reported some closely related nickel-catalyzed borylative cyclization reactions of enynes and allenynes using either HBpin or B$_2$pin$_2$ as the boron source.[35]

In our case, the use of alternative diboron sources B$_2$pin$_2$, B$_2$eg$_2$ and B$_2$neop$_2$ did not achieve borylation at all or showed large quantities of byproducts from oligomerization reactions. We attribute this lack of reactivity to the fact that B$_2$cat$_2$ is the most Lewis acidic diborane(4) under consideration and therefore the most reactive of the diboron reagents used.[36] Furthermore, we have shown recently that bis-NHC adducts of the type (NHC)$_2$·B$_2$(OR)$_4$ are sources of boryl radicals of the type NHC–BR$_2$·, exemplified by Me$_2$Im^{Me}·Bneop· (Me$_2$Im^{Me} = 1,3,4,5-tetramethyl-imidazolin-2-ylidene, neop = neopentylglycolato), which can be used for the transition metal- and additive-free boryl transfer to aryl iodides and bromides giving aryl boronate esters.[37a] We also reported the related phosphine-catalyzed hydroboration of 1,3-diynes with pinacolborane that affords (E)-1-boryl-1,3-enynes and proceeds with excellent selectivity for boron addition to the external carbon of the 1,3-diyne framework.[37b] According to our control experiments, the free carbene ^{i}Pr$_2$Im^{Me} is not a good catalyst for the borylation of alkynes.

Mechanistic investigations – experimental

Interestingly, no major differences in catalytic activity were observed using the nickel alkene complexes **1a–c**, [Ni(^{i}Pr$_2$-Im^{Me})$_2$(η^2-MeC≡CMe)] **14a**, [Ni(^{i}Pr$_2$Im^{Me})$_2$(η^2-cis-(Bcat)(Me)C=C(Me)(Bcat))] **15a** (vide infra) or even the bis-boryl complex **2a** as the catalyst precursor, as all of them appear to serve as a source of [Ni(^{i}Pr$_2$Im^{Me})$_2$]. We were also able to isolate

Scheme 4 Borylation of 2-butyne yielding Z-(Bcat)(Me)C=C(Me)(Bcat) **8**, (Bcat)$_2$(Me)C–C(Me)(Bcat)$_2$ **8a** or E,E-(Bcat)(Me)C=C(Me)–(Me)C=C(Me)(Bcat) **8b**, depending on the stoichiometry used.

analytically pure compounds **4** (60% yield), **7** (65% yield), **8a** (38% yield) and **13** (46% yield) from scaled-up reactions, allowing full characterization, including X-ray diffraction. Additionally, crystals of the compounds **3** (structures of **3** and **4** were reported earlier by Marder *et al.*[13a,38]), **5**, **8**, and **8b** were obtained by slow evaporation of the reaction mixtures (for details see ESI†).

To study the catalytic reaction of 2-butyne, B_2cat_2, and $[Ni(^iPr_2Im^{Me})_2]$ in more detail, we investigated several stoichiometric reactions. Interestingly, the reaction of *cis*-$[Ni(^iPr_2Im^{Me})_2(Bcat)_2]$ **2a** with stoichiometric amounts of 2-butyne did not lead to the *cis*-alkene-1,2-bis(boronate) ester or to the exchange of the boryl ligands with the alkyne to form $[Ni(^iPr_2Im^{Me})_2(\eta^2-MeC≡CMe)]$ **14a**.[22l] Instead, the formation of small amounts of the $[Bcat_2]^-$ anion, traces of a species which was later identified as $[Ni(^iPr_2Im^{Me})_2(\eta^2-cis-(Bcat)(Me)C=C(Me)(Bcat))]$ **15a**, and the slow formation of hexamethylbenzene was detected *via* NMR spectroscopy. Following the complete consumption of 2-butyne after *ca.* 20 h, complex **2a** began to decompose. Although we did not observe the formation of alkyne complex **14a**, the formation of hexamethylbenzene, especially at higher temperatures, suggests that the boryl ligands of **2a** are labile *via* B–B reductive elimination and exchange with the alkyne. However, the reaction of the alkyne complex $[Ni(^iPr_2Im^{Me})_2(\eta^2-MeC≡CMe)]$ **14a**[22l] with B_2cat_2 led to the isolation of the complex of the *cis*-alkene-1,2-bis(boronate) ester $[Ni(^iPr_2Im^{Me})_2(\eta^2-cis-(Bcat)(Me)C=C(Me)(Bcat))]$ **15a** (Scheme 5). This contrasts with the platinum phosphine system, for which Iverson and Smith demonstrated previously that the stoichiometric reaction of $[Pt(PPh_3)_2(\eta^2-H_7C_3C≡CC_3H_7)]$ with B_2cat_2 yields the bis-boryl complex $[Pt(PPh_3)_2(Bcat)_2]$ with extrusion of free alkyne (Scheme 5).[11a] We verified this reactivity by using the octyne complex $[Ni(^iPr_2Im^{Me})_2(\eta^2-H_7C_3C≡CC_3H_7)]$ **14b**, which led to the isolation of $[Ni(^iPr_2Im^{Me})_2(\eta^2-cis-(Bcat)(H_7C_3)C=C(C_3H_7)(Bcat))]$ **15b** (Scheme 5). These borylation reactions of the alkyne coordinated at nickel are quantitative if performed in an NMR tube.

Complexes **15a** and **15b** were isolated as orange to brown solids and were completely characterized using IR- and NMR-

spectroscopy, elemental analysis, and X-ray diffraction. The reduction of symmetry on going from **2a** (pseudo-C_{2v}) to **15a** and **15b** (pseudo-C_s) is reflected in the resonances in the ^1H and $^{13}C\{^1H\}$ NMR spectra of these complexes, which are doubled. The olefinic carbon atoms of the alkene ligand were not detected in the $^{13}C\{^1H\}$ NMR spectra due to the quadrupolar coupling to boron, but were assigned from an HMBC spectrum to be at 40.0 ppm (**15a**) and at 47.3 ppm (**15b**). One broad resonance was observed at 33.3 ppm (**15a**) and 31.9 ppm (**15b**) for the boryl substituents in the $^{11}B\{^1H\}$ NMR spectrum, which are clearly distinct from the resonance of **2a** at 48.7 ppm.

Crystals of **15a** and **15b** suitable for X-ray diffraction were obtained from saturated hexane solutions of the compounds at −30 °C (Fig. 4). The complexes crystallize in the monoclinic space groups $P2_1/c$ (**15a**) and $P2_1/n$ (**15b**). Both complexes adopt a pseudo-trigonal planar structure with Ni–C_{NHC} distances of 1.9454(14)–1.9560(13) Å in a typical range.[22] The C3–C4 distances of the coordinated alkene of 1.453(2) Å (**15a**) and 1.4550(17) Å (**15b**) are in line with those of coordinated olefins reported previously[22a,j] and are much larger compared to those of alkyne complexes (*c.f.* **14a**: 1.285(2) Å).[22l] Both olefin ligands are distorted in such a way that one of the electron-deficient boryl substituents can interact with the electron-rich nickel center (see ESI Fig. S15 and S16†), which results in very different Ni⋯B distances of 2.3694(16) Å (Ni1–B2) and 3.0525(19) Å (Ni1–B1) for complex **15a** and 2.3376(14) Å (Ni1–B2) and 3.0262(14) Å (Ni1–B1) for complex **15b**, respectively. The formation of **15a** and **15b** indicates that the catalytic bis-borylation of alkynes at d^{10}-$[Ni(^iPr_2Im^{Me})_2]$ most likely proceeds *via* a different mechanistic pathway than reported previously for the d^{10}-$[PtL_n]$ platinum system. However, the addition of 2-butyne to **15a** did not lead to the extrusion of the borylation product and regeneration of the alkyne complex **14a** even at higher temperatures, but to formation of hexamethylbenzene.

Mechanistic investigations – DFT calculations

By combining the results obtained from stoichiometric reactions with additional DFT computations, we were able to rationalize the formation of the borylated products **8**, **8a**, and **8b** from 2-butyne, B_2cat_2, and $[Ni(^iPr_2Im^{Me})_2]$. Our proposed
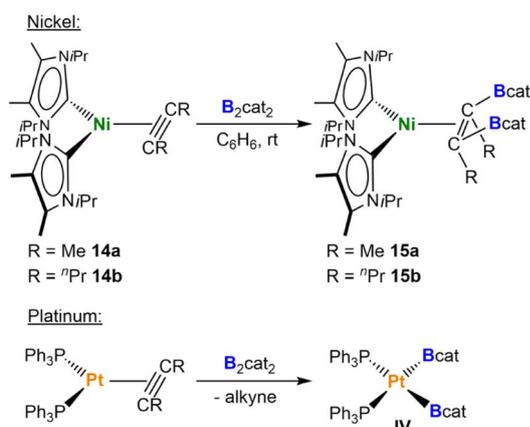
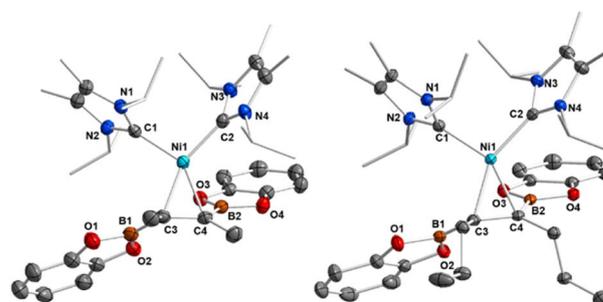**Scheme 5** Reactivity of NHC nickel alkyne complexes and platinum phosphine alkyne complexes with B_2cat_2.

Fig. 4 Molecular structures of $[Ni(^iPr_2Im^{Me})_2(\eta^2-cis-(Bcat)(Me)C=C(Me)(Bcat))]$ **15a** (left) and $[Ni(^iPr_2Im^{Me})_2(\eta^2-cis-(Bcat)(H_7C_3)C=C(C_3H_7)(Bcat))]$ **15b** (right) in the solid state (ellipsoids shown at 50% probability level). Hydrogen atoms have been omitted for clarity. For selected bond lengths and angles see ESI Fig. S15 and S16.†
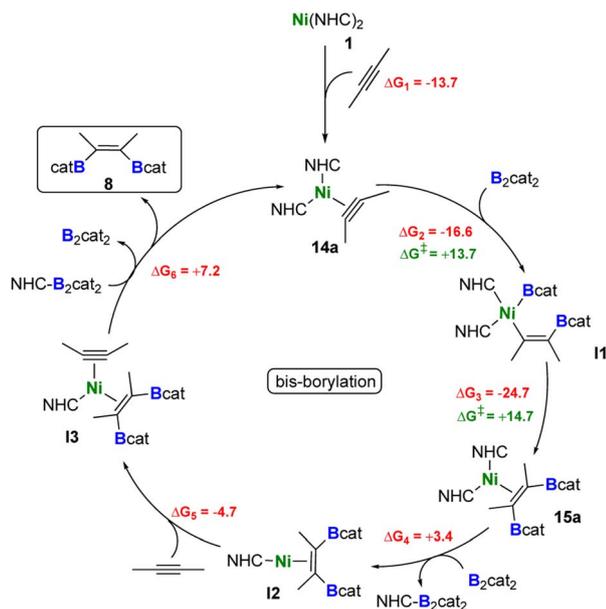
Scheme 6 Proposed catalytic cycle for the formation of **8**. Reaction free energies (kcal mol^{-1}) calculated at the DFT level are shown in red, while energy barriers are shown in green (see ESI† for more details).

catalytic cycles are shown in Schemes 6 (bis-borylation), 7 (tetra-borylation), and 8 (alkyne-coupling); for a comparison to the well-known platinum catalysis see ESI, Fig. S1.† Initially, [Ni(^{i}Pr$_2$Im^{Me})$_2$] **1** reacts with 2-butyne to form the alkyne complex [Ni(^{i}Pr$_2$Im^{Me})$_2$(η^2-MeC≡CMe)] **14a** (ΔG_1 =

−13.7 kcal mol^{-1}), which is competitive to the reaction with B$_2$cat$_2$ ($\Delta G_{1'}$ = −17.5 kcal mol^{-1}).

The next steps leading to [Ni(^{i}Pr$_2$Im^{Me})$_2$(η^2-cis-(Bcat)(Me)C═C(Me)(Bcat))] **15a** are crucial to understand the formation of new tetra-borylation and alkyne-coupling products and the different reaction pathways the system can enter. A detailed energy profile of the mechanistic pathway for the addition of B$_2$cat$_2$ to the alkyne complex **14a** to yield **15a** is therefore pre-sented in Fig. 5. The DFT calculations show that the barrier for the direct addition of B$_2$cat$_2$ to the coordinated alkyne is too high in energy ($\Delta G^{\ddagger}$ = +32.0 kcal mol^{-1}, see **TS1′** in Fig. 5). Interestingly, oxidative addition of B$_2$cat$_2$ to the alkyne complex **14** to yield a nickel(IV) intermediate is sterically hindered and thus also out of reach. Alternatively, **15a** is formed by insertion of B$_2$cat$_2$ into a Ni–C bond maintaining the B–B bond ($\Delta G^{\ddagger}$ = +13.7 kcal mol^{-1}). This σ-complex assisted methathesis (σ-CAM)-type[39] insertion leads to a five-membered NiC$_2$B$_2$ inter-mediate **B** that exergonically isomerizes to a relatively stable nickel monoboryl vinyl complex **I1** (ΔG = −16.6 kcal mol^{-1}). The next step of the sequence is reductive elimination of the vinyl and the boryl substituent of **I1** to yield the complex of the cis-alkene-1,2-bis(boronate) ester [Ni(^{i}Pr$_2$Im^{Me})$_2$(η^2-cis-(Bcat)(Me)C═C(Me)(Bcat))] **15a**. The barrier to pass transition state **TS3** yielding the thermodynamically highly favored product **15a** is calculated to be $\Delta G^{\ddagger}$ = +14.7 kcal mol^{-1} and, thus, in accordance with our experimental findings and surmountable under our reaction conditions. The direct release of bis-borylation product **8** from **15a** is rather endergonic (ΔG = +19.6 kcal mol^{-1}) and, therefore, we propose that in the next

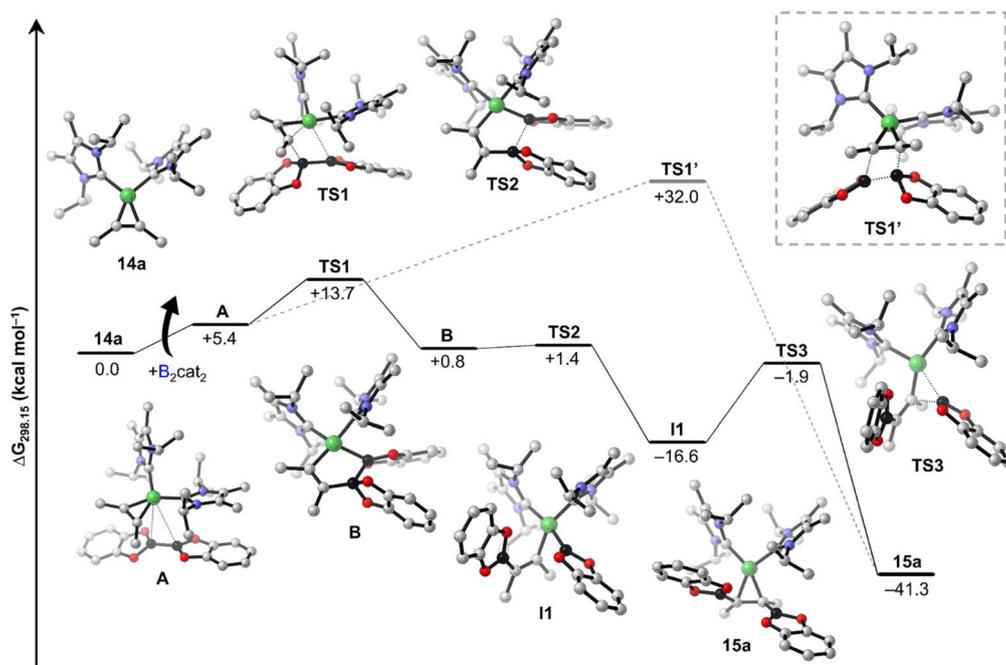**Fig. 5** Free energy profile of the proposed mechanistic pathway for the addition of B$_2$cat$_2$ to the alkyne complex [Ni(^{i}Pr$_2$Im^{Me})$_2$(η^2-MeC≡CMe)] **14a** to yield [Ni(^{i}Pr$_2$Im^{Me})$_2$(η^2-cis-(Bcat)(Me)C═C(Me)(Bcat))] **15a**. Black lines connect the preferred pathway, while dashed lines indicate a pathway involving a high-energy transition state **TS1′**. Calculated free energies (kcal mol^{-1}) are at the SMD(benzene)/PBE0-D3(BJ)/def2-TZVPP//PBE0-D3(BJ)/def2-SVP/def2-TZVP(Ni) level of theory. Hydrogen atoms are omitted for clarity.
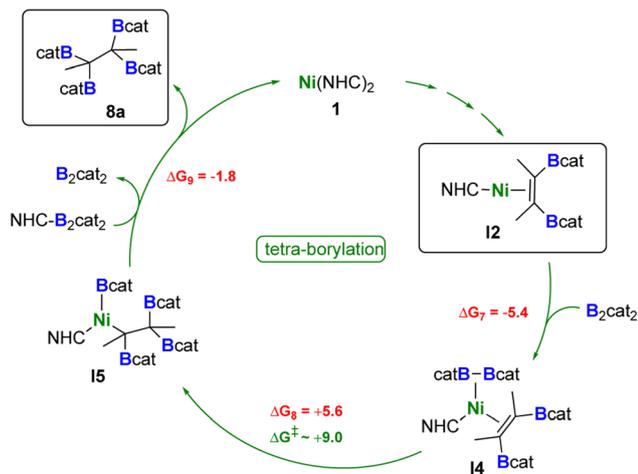
Scheme 7 Proposed catalytic cycle for the formation of **8a**. Reaction free energies (kcal mol^{-1}) calculated at the DFT level are shown in red, while energy barriers are shown in green (see ESI† for more details).

step an NHC is transferred from **15a** to another B_2cat_2 molecule (Scheme 6, $\Delta G_4 = +3.4$ kcal mol^{-1}). This leads to the mono-NHC intermediate **I2**. Addition of an alkyne to **I2** leads to **I3** and is slightly exergonic ($\Delta G_5 = -4.7$ kcal mol^{-1}). The release of **8** from **I3** is then mediated by a transfer of the NHC ligand from the ligand-activated B_2cat_2 species, whose step is endergonic by $\Delta G_6 = +7.2$ kcal mol^{-1} and regenerates **14a** and B_2cat_2.

The catalytic cycle leading to the tetra-borylated product **8a** is shown in Scheme 7. The mono-NHC intermediate **I2** can react

with B_2cat_2 leading exergonically to **I4** ($\Delta G_7 = -5.4$ kcal mol^{-1}). This species can undergo facile B–B bond dissociation and formation of the nickel monoboryl species **I5** ($\Delta G_8 = +5.6$ kcal mol^{-1}), where the other boryl group is transferred to the alkene moiety. Although a transition state for this reaction step was not successfully found despite our best efforts, relaxed scan calculations revealed that the energy barrier for this transformation is around 9 kcal mol^{-1} (see Fig. S91 in the ESI†).

The release of the tetra-borylated product **8a** ($\Delta G_9 = -1.8$ kcal mol^{-1}) is then mediated by the NHC-activated B_2cat_2 species, with further regeneration of B_2cat_2 and **1**.

We found that the formation of the alkyne coupling product **8b** can occur *via* two competitive pathways, starting either from nickel monoboryl vinyl complex **I1** (see blue cycle in Scheme 8) or from **15a** (see pink cycle in Scheme 8). Assuming that bis-borylation is very fast and all B_2cat_2 has been consumed, **15a** can transfer an NHC to the product **8** (NHC-prod, $\Delta G_{10} = +3.7$ kcal mol^{-1}), which would again lead to **I2**. As already discussed, this intermediate can be converted to **I3** after addition of an alkyne.

Details of the alkyne coupling step going from **I3** to **I8** are shown in Fig. 6. We propose that the alkyne coupling can start from **I3** with insertion of 2-butyne into the Ni–C bond of the coordinated *cis*-alkene-1,2-bis(boronate) ester, which leads to **I6** ($\Delta G_{11} = +2.0$ kcal mol^{-1}), a bis-borylated unsymmetrical met-allacyclopentene, energetically close in energy to **I3**. **I6** then undergoes a subsequent 1,3-shift of a boryl group leading to the symmetrical metallacyclopentene complex **I7** ($\Delta G_{12} = -14.1$ kcal mol^{-1}). This concerted 1,3-shift of the boryl
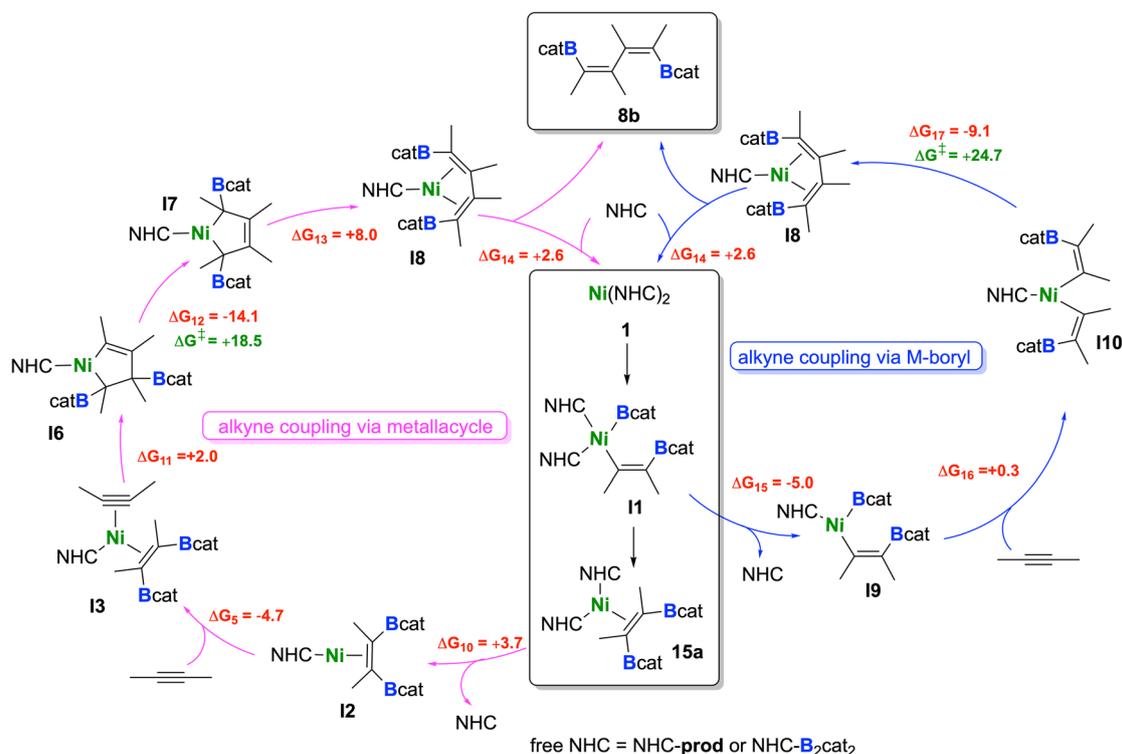
Scheme 8 Proposed catalytic cycles for the formation of **8b**. Reaction free energies (kcal mol^{-1}) calculated at the DFT level are shown in red, while energy barriers are shown in green (see ESI† for more details).
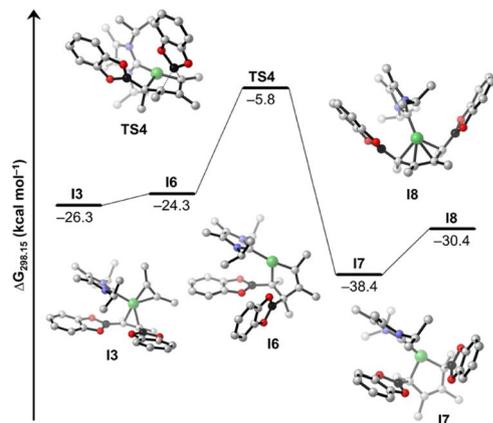
Fig. 6 Free energy profile of the proposed mechanistic pathway from **I3** to **I8**. Calculated free energies (kcal mol^{-1}) are at the SMD(benzene)/PBE0-D3(BJ)/def2-TZVPP//PBE0-D3(BJ)/def2-SVP/def2-TZVP(Ni) level of theory, and are referenced to the resting state **14a** + C_2Me_2 + B_2cat_2. Hydrogen atoms are omitted for clarity.

substituent *via* **TS4** is associated with a relatively low barrier ($\Delta G^{\ddagger} = +18.5$ kcal mol^{-1}). The resulting metallacyclopentene complex **I7** rearranges to a 1,4-bis-boryl butadiene complex **I8**, which is stabilized by a mono-NHC nickel moiety ($\Delta G_{13} = +8.0$ kcal mol^{-1}). The release of **8b** is then facilitated by re-coordination of an NHC to the Ni center ($\Delta G_{14} = +2.6$ kcal mol^{-1}) regenerating complex **1**.

Following the blue reaction path of Scheme 8, dissociation of an NHC from **I1** (and/or transfer to any boron compound) leads to the mono-NHC-stabilized boryl species **I9** ($\Delta G_{15} = -5.0$ kcal mol^{-1} considering NHC dissociation), a step which is well known from platinum chemistry (see ESI Scheme S1†). Surprisingly, formation of **I9** from **I1** is exergonic even considering just the dissociation of the NHC ligand. This happens because the formally three-coordinate Ni center of **I9** is
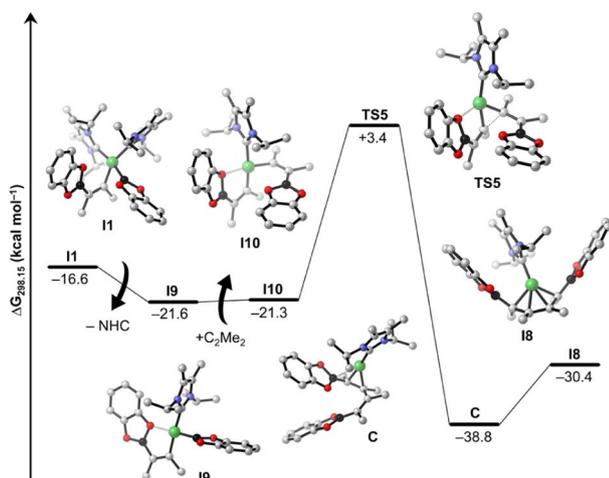
stabilized by interaction with an oxygen atom of the Bcat group (Ni⋯O contact in the optimized structure: 2.056 Å). However, reductive elimination of the *cis*-alkene-1,2-bis(boronate) ester from **I9** is high in energy and interception of this intermediate by another alkyne gives a mixed substituted alkyne boryl vinyl complex. All attempts to optimize this latter structure failed, as the Bcat group at nickel undergoes immediately facile transfer to the vinyl moiety so that reductive elimination to form intermediate **I3** takes place. On the other hand, insertion of the coordinated alkyne into the Ni–B bond of **I9** yields the nickel bis(vinyl) complex **I10** ($\Delta G_{16} = +0.3$ kcal mol^{-1}). Subsequent C–C reductive elimination from **I10** *via* **TS5** (Fig. 7, $\Delta G^{\ddagger} = +24.7$ kcal mol^{-1}) yields the NHC–Ni butadiene **I8** ($\Delta G_{18} = -9.1$ kcal mol^{-1}), which releases the product **8b**, similarly as computed for the other pathway. The results indicate that both pathways are competitive and accessible under the reaction conditions employed, with a preference for the pink cycle due to its lower energy barrier.

Conclusions

It has been shown over the last decades that transition metal poly-boryl complexes play pivotal roles and are key intermediates in many borylation processes. Such complexes were typically associated with noble metals but, as first-row d-block metals are less toxic, less expensive, Earth-abundant, and environmentally benign, they are very attractive alternatives to these expensive noble metals. Nickel boryl complexes are generally considered to be elusive, in contrast to other 3d-metals such as iron, cobalt, or copper. We report herein the first nickel bis-boryl complexes *cis*-[Ni(^{i}Pr$_2$Im^{Me})$_2$(Bcat)$_2$] **2a**, *cis*-[Ni(^{i}Pr$_2$Im^{Me})$_2$(Bpin)$_2$] **2b** and *cis*-[Ni(^{i}Pr$_2$Im^{Me})$_2$(Beg)$_2$] **2c**, which can be synthesized from the reaction of a source of [Ni(^{i}Pr$_2$Im^{Me})$_2$] with the diboron(4) compounds B_2cat_2, B_2pin_2, and B_2eg_2. Key to the successful synthesis was the choice of the NHC used, showing the right stereo-electronic properties. Whereas *cis*-[Ni(^{i}Pr$_2$Im^{Me})$_2$(Bcat)$_2$] **2a** was isolated as a pale brown solid in 58% yield, the reaction with either B_2pin_2 or B_2eg_2 instead of B_2cat_2 did not proceed quantitatively at room temperature, as observed by NMR spectroscopy. X-ray diffraction studies on **2a–c** and DFT calculations on **2a** suggest that a delocalized, multicenter bonding scheme best describes the bonding situation of the NiB$_2$ moiety in these complexes, which is reminiscent of the bonding situation in "non-classical" H$_2$ complexes.

We also demonstrate that [Ni(^{i}Pr$_2$Im^{Me})$_2$] catalyst precursors provide excellent catalytic activity for the diboration of alkynes under mild conditions, using B_2cat_2 as the boron source. Beside the well-known *cis*-alkene-1,2-bis(boronate) esters, the formation of C–C coupled borylation products such as **8b**, **12a**, and **12b** as well as tetra-borylated products such as **8a** and **13** were observed or produced as main products of the reaction, which significantly expands the (poly)borylation of alkynes and the scope of accessible boron compounds for further transformations. Therefore, we demonstrated that these 3d metal catalysts provide the potential for new selectivities for the borylation of alkynes compared to the well-established catalysts.

Fig. 7 Free energy profile of the proposed mechanistic pathway from **I1** to **I8**. Calculated free energies (kcal mol^{-1}) are at the SMD(benzene)/PBE0-D3(BJ)/def2-TZVPP//PBE0-D3(BJ)/def2-SVP/def2-TZVP(Ni) level of theory, and are referenced to the resting state **14a** + C_2Me_2 + B_2cat_2. Hydrogen atoms are omitted for clarity.

Mechanistic investigations supported by DFT calculations revealed significant differences between our NHC nickel system and the well-established platinum-phosphine chemistry. The formation of borylated alkene π-complexes **15a** and **15b** as catalytic intermediates is crucial to understand the new catalytic pathway and the formation of new borylation products. Further studies concerning the reactivity of nickel bis-boryl complexes are currently under investigation.

Data availability

Additional data and spectra, crystallographic data, NMR spectra, details on the DFT calculations and Cartesian coordinates of the DFT optimized structures can be found in the ESI.†

Author contributions

L. T., U. R., T. B. M., and F. F. conceived the project. L. T. performed all the experiments. F. F. performed the quantum chemical calculations. L. T., F. F., T. B. M., and U. R. wrote the manuscript. All authors discussed the results and contributed to the final manuscript.

Conflicts of interest

There are no conflicts to declare.

Acknowledgements

References

1 (a) H. C. Brown, *Science*, 1980, **210**, 485–492; (b) N. Miyarura, *Top. Curr. Chem.*, 2002, **219**, 11–59; (c) *Boron compounds, Science of Syntheses*, ed. D. E. Kaufmann and D. S. Matteson, Georg Thieme Verlag, Stuttgart, 2005, vol. 6; (d) *Boronic Acids-Preparation and Applications in Organic Synthesis, Medicine and Materials*, ed. D. G. Hall, Wiley-VCH, Weinheim, Germany, 2nd edn, 2011; (e) E. C. Neeve, S. J. Geier, I. A. I. Mkhalid, S. A. Westcott and T. B. Marder, *Chem. Rev.*, 2016, **116**, 9091–9161; (f) M. Wang and Z. Shi, *Chem. Rev.*, 2020, **120**, 7348–7398; (g) Y.-M. Tian, X.-N. Guo, H. Braunschweig, U. Radius and T. B. Marder, *Chem. Rev.*, 2021, **121**, 3561–3597; (h) S. K. Bose, L. Mao, L. Kuehn, U. Radius, J. Nekvinda, W. L. Santos, S. A. Westcott, P. G. Steel and T. B. Marder, *Chem. Rev.*, 2021, **121**, 13238–13341; (i) J. Hu, M. Ferger, Z. Shi and T. B. Marder, *Chem. Soc. Rev.*, 2021, **50**, 13129–13188; (j) S. Manna, K. K. Das, S. Nandy, D. Aich, S. Paul and S. Panda, *Coord. Chem. Rev.*, 2021, **448**, 214165.

2 (a) T. Ishiyama, M. Murata and N. Miyaura, *J. Org. Chem.*, 1995, **60**, 7508–7510; (b) L. T. Pilarski and K. J. Szabó, *Angew. Chem., Int. Ed.*, 2011, **50**, 8230–8232; (c) M. Murata, *Heterocycles*, 2012, **85**, 1795–1819; (d) C. M. Vogels and S. A. Westcott, *ChemCatChem*, 2012, **4**, 47–49; (e) W. K. Chow, O. Y. Yuen, P. Y. Choy, C. M. So, C. P. Lau, W. T. Wong and F. Y. Kwong, *RSC Adv.*, 2013, **3**, 12518–12539; (f) K. Kubota, H. Iwamoto and H. Ito, *Org. Biomol. Chem.*, 2017, **15**, 285–300; (g) Y. P. Budiman, S. A. Westcott, U. Radius and T. B. Marder, *Adv. Synth. Catal.*, 2021, **363**, 2224–2255.

3 (a) I. Beletskaya and A. Pelter, *Tetrahedron*, 1997, **53**, 4957–5026; (b) V. Lillo, A. Bonet and E. Fernández, *Dalton Trans.*, 2009, 2899–2908; (c) J. Takaya and N. Iwasawa, *ACS Catal.*, 2012, **2**, 1993–2006; (d) H. Wen, G. Liu and Z. Huang, *Coord. Chem. Rev.*, 2019, **386**, 138–153; (e) W. Fan, L. Li and G. Zhang, *J. Org. Chem.*, 2019, **84**, 5987–5996; (f) O. Salvadó and E. Fernández, *Molecules*, 2020, **25**, 1758; (g) X. Wang, Y. Wang, W. Huang, C. Xia and L. Wu, *ACS Catal.*, 2021, **11**, 1–18.

4 (a) T. B. Marder and N. C. Norman, *Top. Catal.*, 1998, **5**, 63–73; (b) R. Barbeyron, E. Benedetti, J. Cossy, J.-J. Vasseur, S. Arseniyadis and M. Smietana, *Tetrahedron*, 2014, **70**, 8431–8452; (c) H. Yoshida, *ACS Catal.*, 2016, **6**, 1799–1811; (d) E. Buñuel and D. J. Cárdenas, *Eur. J. Org. Chem.*, 2016, 5446–5464; (e) M. B. Ansell, O. Navarro and J. Spencer, *Coord. Chem. Rev.*, 2017, **336**, 54–77; (f) F. Zhao, X. Jia, P. Li, J. Zhao, Y. Zhou, J. Wang and H. Liu, *Org. Chem. Front.*, 2017, **4**, 2235–2255; (g) E. Buñuel and D. J. Cárdenas, *Chem.–Eur. J.*, 2018, **24**, 11239–11244; (h) J. Carreras, A. Caballero and P. J. Perez, *Chem.–Asian J.*, 2019, **14**, 329–343.

5 (a) T. Ishiyama and N. Miyaura, *J. Organomet. Chem.*, 2003, **680**, 3–11; (b) I. A. I. Mkhalid, J. H. Barnard, T. B. Marder, J. M. Murphy and J. F. Hartwig, *Chem. Rev.*, 2010, **110**, 890–931; (c) J. F. Hartwig, *Chem. Soc. Rev.*, 2011, **40**, 1992–2002; (d) J. F. Hartwig, *Acc. Chem. Res.*, 2012, **45**, 864–873; (e) A. Ros, R. Fernández and J. M. Lassaletta, *Chem. Soc. Rev.*, 2014, **43**, 3229–3243; (f) J. F. Hartwig, *J. Am. Chem. Soc.*, 2016, **138**, 2–24; (g) Y. Ping, L. Wang, Q. Ding and Y. Peng, *Adv. Synth. Catal.*, 2017, **359**, 3274–3291; (h) T. Gensch, M. J. James, T. Dalton and F. Glorius, *Angew. Chem., Int. Ed.*, 2018, **57**, 2296–2306; (i) Y. Shi, Q. Gao and S. Xu, *Synlett*, 2019, **30**, 2107–2112; (j) E. Fernandez, *Top. Organomet. Chem.*, 2021, **69**, 207–225.

6 (a) G. J. Irvine, M. J. Lesley, T. B. Marder, N. C. Norman, C. R. Rice, E. G. Robins, W. R. Roper, G. R. Whittell and L. J. Wright, *Chem. Rev.*, 1998, **98**, 2685–2722; (b) H. Braunschweig, *Angew. Chem., Int. Ed.*, 1998, **37**, 1786–1801; (c) H. Braunschweig and M. Colling, *Coord. Chem. Rev.*, 2001, **223**, 1–51; (d) S. Aldridge and D. L. Coombs, *Coord. Chem. Rev.*, 2004, **248**, 535–559; (e) H. Braunschweig, C. Kollann and D. Rais, *Angew. Chem., Int. Ed.*, 2006, **45**, 5254–5274; (f) D. L. Kays and S. Aldridge, *Struct. Bond.*, 2008, **130**, 29–122; (g) U. Kaur, K. Saha, S. Gayen and S. Ghosh, *Coord. Chem. Rev.*, 2021, **446**, 214106.

7 (a) T. Ishiyama and N. Miyaura, *J. Organomet. Chem.*, 2000, **611**, 392–402; (b) N. Miyaura, *Bull. Chem. Soc. Jpn.*, 2008, **81**, 1535–1553; (c) L. Dang, Z. Lin and T. B. Marder, *Chem. Commun.*, 2009, 3987–3995; (d) X. Guo, T. Yang, F. K. Sheong and Z. Lin, *ACS Catal.*, 2021, **11**, 5061–5068.

8 (a) P. Nguyen, H. P. Blom, S. A. Westcott, N. J. Taylor and T. B. Marder, *J. Am. Chem. Soc.*, 1993, **115**, 9329–9330; (b) R. T. Baker, J. C. Calabrese, S. A. Westcott, P. Nguyen and T. B. Marder, *J. Am. Chem. Soc.*, 1993, **115**, 4367–4368; (c) K. Burgess, W. A. Van der Donk, S. A. Westcott, T. B. Marder, R. T. Baker and J. C. Calabrese, *J. Am. Chem. Soc.*, 1992, **114**, 9350–9359.

9 (a) T. Ishiyama, J. Takagi, K. Ishida, N. Miyaura, N. R. Anastasi and J. F. Hartwig, *J. Am. Chem. Soc.*, 2002, **124**, 390–391; (b) J.-Y. Cho, M. K. Tse, D. Holmes, R. E. Maleczka Jr and M. R. Smith III, *Science*, 2002, **295**, 305–308; (c) M. A. Larsen and J. F. Hartwig, *J. Am. Chem. Soc.*, 2014, **136**, 4287–4299.

10 (a) A. K. Cook, S. D. Schimler, A. J. Matzger and M. S. Sanford, *Science*, 2016, **351**, 1421–1424; (b) K. T. Smith, S. Berritt, M. González-Moreiras, S. Ahn, M. R. Smith, M.-H. Baik and D. J. Mindiola, *Science*, 2016, **351**, 1424–1427; (c) S. Ahn, D. Sorsche, S. Berritt, M. R. Gau, D. J. Mindiola and M.-H. Baik, *ACS Catal.*, 2018, **8**, 10021–10031.

11 (a) C. N. Iverson and M. R. Smith III, *J. Am. Chem. Soc.*, 1995, **117**, 4403–4404; (b) C. Borner and C. Kleeberg, *Eur. J. Inorg. Chem.*, 2014, 2486–2489.

12 (a) T. Ishiyama, N. Matsuda, N. Miyaura and A. Suzuki, *J. Am. Chem. Soc.*, 1993, **115**, 11018–11019; (b) T. Ishiyama, N. Matsuda, M. Murata, F. Ozawa, A. Suzuki and N. Miyaura, *Organometallics*, 1996, **15**, 713–720; (c) C. N. Iverson and M. R. Smith, *Organometallics*, 1996, **15**, 5155–5165; (d) Q. Cui, D. G. Musaev and K. Morokuma, *Organometallics*, 1998, **17**, 742–751.

13 (a) G. Lesley, P. Nguyen, N. J. Taylor, T. B. Marder, A. J. Scott, W. Clegg and N. C. Norman, *Organometallics*, 1996, **15**, 5137–5154; (b) R. Ll. Thomas, F. E. S. Souza and T. B. Marder, *Dalton Trans.*, 2001, 1650–1656.

14 (a) T. Ishiyama and N. Miyaura, *Chem. Rec.*, 2004, **4**, 271–280; (b) M. W. Carson, M. W. Giese and M. J. Coghlan, *Org. Lett.*, 2008, **10**, 2701–2704; (c) K. Yavari, S. Moussa, B. Ben Hassine, P. Retailleau, A. Voituriez and A. Marinetti, *Angew. Chem., Int. Ed.*, 2012, **51**, 6748–6752; (d) Q.-X. Lin and T.-L. Ho, *Tetrahedron*, 2013, **69**, 2996–3001; (e) M. W. Carson, J. G. Luz, C. Suen, C. Montrose, R. Zink, X. Ruan, C. Cheng, H. Cole, M. D. Adrian, D. T. Kohlman, T. Mabry, N. Snyder, B. Condon, M. Maletic, D. Clawson, A. Pustilnik and M. J. Coghlan, *J. Med. Chem.*, 2014, **57**, 849–860; (f) J. Yang, M. Chem, J. Ma, W. Huang, H. Zhu, Y. Huang and W. Wang, *J. Mater. Chem. C*, 2015, **3**, 10074–10078.

15 (a) C. Kleeberg, L. Dang, Z. Lin and T. B. Marder, *Angew. Chem., Int. Ed.*, 2009, **48**, 5350–5354; (b) C.-T. Yang, Z.-Q. Zhang, H. Tajuddin, C.-C. Wu, J. Liang, J.-H. Liu, Y. Fu, M. Czyzewska, P. G. Steel, T. B. Marder and L. Liu, *Angew. Chem., Int. Ed.*, 2012, **51**, 528–532; (c) S. K. Bose, S. Brand, H. O. Omoregie, M. Haehnel, J. Maier, G. Bringmann and T. B. Marder, *ACS Catal.*, 2016, **6**, 8332–8335; (d) D. Hemming, R. Fritzemeier, S. A. Westcott, W. L. Santos and P. G. Steel, *Chem. Soc. Rev.*, 2018, **47**, 7477–7494; (e) L. Kuehn, M. Huang, U. Radius and T. B. Marder, *Org. Biomol. Chem.*, 2019, **17**, 6601–6606; (f) B. S. Takale, R. R. Thakore, E. Etemadi-Davan and B. H. Lipshutz, *Beilstein J. Org. Chem.*, 2020, **16**, 691–737; (g) A. Whyte, A. Torelli, B. Mirabi, A. Zhang and M. Lautens, *ACS Catal.*, 2020, **10**, 11578–11622.

16 (a) J. Zhou, M. W. Kuntze-Fechner, R. Bertermann, U. S. D. Paul, J. H. Berthel, A. Friedrich, Z. Du, T. B. Marder and U. Radius, *J. Am. Chem. Soc.*, 2016, **138**, 5250–5253; (b) Y.-M. Tian, X.-N. Guo, M. Kuntze-Fechner, I. Krummenacher, H. Braunschweig, U. Radius, A. Steffen and T. B. Marder, *J. Am. Chem. Soc.*, 2018, **140**, 17612–17623; (c) M. W. Kuntze-Fechner, H. Verplancke, L. Tendera, M. Diefenbach, I. Krummenacher, H. Braunschweig, T. B. Marder, M. C. Holthausen and U. Radius, *Chem. Sci.*, 2020, **11**, 11009–11023; (d) L. Kuehn, D. G. Jammal, K. Lubitz, T. B. Marder and U. Radius, *Chem.–Eur. J.*, 2019, **25**, 9514–9521; (e) Y.-M. Tian, X.-N. Guo, I. Krummenacher, Z. Wu, J. Nitsch, H. Braunschweig, U. Radius and T. B. Marder, *J. Am. Chem. Soc.*, 2020, **142**, 18231–18242; (f) Y.-M. Tian, X.-N. Guo, Z. Wu, A. Friedrich, S. A. Westcott, H. Braunschweig, U. Radius and T. B. Marder, *J. Am. Chem. Soc.*, 2020, **142**, 13136–13144.

17 The reaction of [Ni(Cy₂Im)₂(Ar)Cl] with stoichiometric amounts of B₂pin₂ at room temperature led to a resonance at 44.5 ppm in the ¹¹B{¹H} NMR spectrum of the reaction mixture which indicated the formation of a nickel-boryl complex, see the ESI† of ref. 16 d.

18 (a) J. F. Hartwig and S. Huber, *J. Am. Chem. Soc.*, 1993, **115**, 4908–4909; (b) X. He and J. F. Hartwig, *Organometallics*, 1996, **15**, 400–407; (c) K. M. Waltz, C. N. Muhoro and J. F. Hartwig, *Organometallics*, 1999, **18**, 3383–3393; (d) S. Aldridge, R. J. Calder, R. E. Baghurst, M. E. Light and M. B. Hursthouse, *J. Organomet. Chem.*, 2002, **649**, 9–14; (e) A. Rossin, S. Aldridge and L.-l. Ooi, *Appl. Organomet. Chem.*, 2005, **19**, 181–182; (f) T. J. Mazzacano and N. P. Mankad, *Chem. Commun.*, 2015, **51**, 5379–5382; (g) R. B. Bedford, P. B. Brenner, E. Carter, T. Gallagher, D. M. Murphy and D. R. Pye, *Organometallics*, 2014, **33**, 5940–5943; (h) T. Dombray, C. G. Werncke, S. Jiang, M. Grellier, L. Vendier, S. Bontemps, J.-B. Sortais, S. Sabo-Etienne and C. Darcel, *J. Am. Chem. Soc.*, 2015, **137**, 4062–4065; (i) L. Vondung, N. Frank, M. Fritz, L. Alig and R. Langer, *Angew. Chem., Int. Ed.*, 2016, **55**, 14450–14454; (j) K. Nakajima, T. Kato and Y. Nishibayashi, *Org. Lett.*, 2017, **19**, 4323–4326; (k) T. Kato, S. Kuriyama, K. Nakajima and Y. Nishibayashi, *Chem.–Asian J.*, 2019, **14**, 2097–2101.

19 (a) C. Dai, G. Stringer, J. F. Corrigan, N. J. Taylor, T. B. Marder and N. C. Norman, *J. Organomet. Chem.*, 1996, **513**, 273–275; (b) C. J. Adams, R. A. Baber, A. S. Batsanov, G. Bramham, J. P. Charmant, M. F. Haddow, J. A. K. Howard, W. H. Lam, Z. Lin, T. B. Marder, N. C. Norman and A. G. Orpen, *Dalton Trans.*, 2006, 1370–

1373; (*c*) J. V. Obligacion, S. P. Semproni and P. J. Chirik, *J. Am. Chem. Soc.*, 2014, **136**, 4133–4136; (*d*) J. V. Obligacion, S. P. Semproni, I. Pappas and P. J. Chirik, *J. Am. Chem. Soc.*, 2016, **138**, 10645–10653; (*e*) S. M. Rummelt, H. Zhong, N. G. Léonard, S. P. Semproni and P. J. Chirik, *Organometallics*, 2019, **38**, 1081–1090; (*f*) R. Arevalo, T. P. Pabst and P. J. Chirik, *Organometallics*, 2020, **39**, 2763–2773; (*g*) W. Drescher, D. Schmitt-Monreal, C. R. Jacob and C. Kleeberg, *Organometallics*, 2020, **39**, 538–543.

20 (*a*) D. S. Laitar, P. Müller and J. P. Sadighi, *J. Am. Chem. Soc.*, 2005, **127**, 17196–17197; (*b*) K. Semba, M. Shinomiya, T. Fujihara, J. Terao and Y. Tsuji, *Chem.–Eur. J.*, 2013, **19**, 7125–7132; (*c*) C. M. Wyss, J. Bitting, J. Bacsa, T. G. Gray and J. P. Sadighi, *Organometallics*, 2016, **35**, 71–74; (*d*) C. Borner, L. Anders, K. Brandhorst and C. Kleeberg, *Organometallics*, 2017, **36**, 4687–4690; (*e*) C. Kleeberg and C. Borner, *Organometallics*, 2018, **37**, 4136–4146; (*f*) W. Drescher and C. Kleeberg, *Inorg. Chem.*, 2019, **58**, 8215–8229; (*g*) W. Drescher, C. Borner and C. Kleeberg, *New J. Chem.*, 2021, **45**, 14957–14964; (*h*) P. Ríos, M. S. See, R. C. Handford, S. J. Teat and T. D. Tilley, *Chem. Sci.*, 2022, **13**, 6619–6625; (*i*) P. M. Rutz, J. Grunenberg and C. Kleeberg, *Organometallics*, 2022, **41**, 3044.

21 (*a*) D. Adhikari, J. C. Huffman and D. J. Mindiola, *Chem. Commun.*, 2007, 4489–4491; (*b*) B. L. Tran, D. Adhikari, H. Fan, M. Pink and D. J. Mindiola, *Dalton Trans.*, 2010, **39**, 358–360; (*c*) T.-P. Lin and J. C. Peters, *J. Am. Chem. Soc.*, 2014, **136**, 13672–13683; (*d*) N. Curado, C. Maya, J. López-Serrano and A. Rodríguez, *Chem. Commun.*, 2014, **50**, 15718–15721; (*e*) P. Ríos, J. Borge, F. Fernández de Córdova, G. Sciortino, A. Lledós and A. Rodríguez, *Chem. Sci.*, 2021, **12**, 2540–2548; (*f*) F. W. Seidel and K. Nozaki, *Angew. Chem., Int. Ed.*, 2022, **61**, e202111691.

22 (*a*) T. Schaub and U. Radius, *Chem.–Eur. J.*, 2005, **11**, 5024–5030; (*b*) T. Schaub, M. Backes and U. Radius, *Organometallics*, 2006, **25**, 4196–4206; (*c*) U. S. D. Paul, C. Sieck, M. Hähnel, K. Hammond, T. B. Marder and U. Radius, *Chem.–Eur. J.*, 2016, **21**, 11005–11014; (*d*) U. S. D. Paul and U. Radius, *Chem.–Eur. J.*, 2017, **23**, 3993–4009; (*e*) U. S. D. Paul and U. Radius, *Organometallics*, 2017, **36**, 1398–1407; (*f*) J. H. J. Berthel, M. W. Kuntze-Fechner and U. Radius, *Eur. J. Inorg. Chem.*, 2019, 2618–2623; (*g*) J. H. J. Berthel, L. Tendera, M. W. Kuntze-Fechner, L. Kuehn and U. Radius, *Eur. J. Inorg. Chem.*, 2019, 3061–3072; (*h*) J. H. J. Berthel, M. J. Krahfuss, U. Radius and Z. Anorg, *Allg. Chem.*, 2020, **646**, 692–704; (*i*) M. J. Krahfuss, J. Nitsch, F. M. Bickelhaupt, T. B. Marder and U. Radius, *Chem.–Eur. J.*, 2020, **26**, 11276–11292; (*j*) L. Tendera, T. Schaub, M. J. Krahfuss, M. W. Kuntze-Fechner and U. Radius, *Eur. J. Inorg. Chem.*, 2020, 3194–3207; (*k*) S. Sabater, D. Schmidt, H. Schmidt nee Schneider, M. Kuntze-Fechner, T. Zell, C. J. Isaac, H. Grieve, W. J. M. Blackaby, J. P. Lowe, S. A. Macgregor, M. F. Mahon, F. M. Miloserdov, N. Rajabi, U. Radius and M. K. Whittlesey, *Chem.–Eur. J.*, 2021, **27**, 13221–13234; (*l*) L. Tendera, M. Helm, M. J. Krahfuss, M. W. Kuntze-Fechner and U. Radius, *Chem.–Eur. J.*, 2021, **27**, 17849–17861.

23 (*a*) S. Würtemberger-Pietsch, U. Radius and T. B. Marder, *Dalton Trans.*, 2016, **45**, 5880–5895; (*b*) S. Pietsch, U. Paul, I. A. Cade, M. J. Ingleson, U. Radius and T. B. Marder, *Chem.–Eur. J.*, 2015, **21**, 9018–9021; (*c*) S. Würtemberger-Pietsch, H. Schneider, T. B. Marder and U. Radius, *Chem.–Eur. J.*, 2016, **22**, 13032–13036; (*d*) M. Eck, S. Würtemberger-Pietsch, A. Eichhorn, J. H. J. Berthel, R. Bertermann, U. S. D. Paul, H. Schneider, A. Friedrich, C. Kleeberg, U. Radius and T. B. Marder, *Dalton Trans.*, 2017, **46**, 3661–3680.

24 (*a*) H. Clavier and S. P. Nolan, *Chem. Commun.*, 2010, **46**, 841–861; (*b*) S. Felten, S. F. Marshall, A. J. Groom, R. T. Vanderlinden, R. M. Stolley and J. Louie, *Organometallics*, 2018, **37**, 3687–3697.

25 (*a*) W. Clegg, F. J. Lawlor, G. Lesley, T. B. Marder, N. C. Norman, A. G. Orpen, M. J. Quayle, C. R. Rice, A. J. Scott and F. E. S. Souza, *J. Organomet. Chem.*, 1998, **550**, 183–192; (*b*) J. Zhu, Z. Lin and T. B. Marder, *Inorg. Chem.*, 2005, **44**, 9384–9390; (*c*) H. Braunschweig, P. Brenner, A. Müller, K. Radacki, D. Rais and K. Uttinger, *Chem.–Eur. J.*, 2007, **13**, 7171–7176.

26 (*a*) T. Zell, T. Schaub, K. Radacki and U. Radius, *Dalton Trans.*, 2011, **40**, 1852–1854; (*b*) C. Hauf, J. E. Barquera-Lozada, P. Meixner, G. Eickerling, S. Altmannshofer, D. Stalke, T. Zell, D. Schmidt, U. Radius and W. Scherer, *Z. Anorg. Allg. Chem.*, 2013, **639**, 1996–2004; (*c*) D. Schmidt, T. Zell, T. Schaub and U. Radius, *Dalton Trans.*, 2014, **43**, 10816–10827.

27 W. Clegg, M. R. J. Elsegood, F. J. Lawlor, N. C. Norman, N. L. Pickett, E. G. Robins, A. J. Scott, P. Nguyen, N. J. Taylor and T. B. Marder, *Inorg. Chem.*, 1998, **37**, 5289–5293.

28 (*a*) I. Mayer, *Chem. Phys. Lett.*, 1983, **97**, 270–274; (*b*) I. Mayer, *Int. J. Quantum Chem.*, 1984, **26**, 151–154.

29 G. Knizia, *J. Chem. Theory Comput.*, 2013, **9**, 4834–4843.

30 (*a*) M. Ernzerhof and G. E. Scuseria, *J. Chem. Phys.*, 1999, **110**, 5029–5036; (*b*) C. Adamo and V. Barone, *J. Chem. Phys.*, 1999, **110**, 6158–6170; (*c*) S. Grimme, J. Antony, S. Ehrlich and H. Krieg, *J. Chem. Phys.*, 2010, **132**, 154104; (*d*) S. Grimme, S. Ehrlich and L. Goerigk, *J. Comput. Chem.*, 2011, **32**, 1456–1465; (*e*) F. Weigend and R. Ahlrichs, *Phys. Chem. Chem. Phys.*, 2005, **7**, 3297–3305.

31 M. B. Ansell, V. H. Menezes da Silva, G. Heerdt, A. A. C. Braga, J. Spencer and O. Navarro, *Catal. Sci. Technol.*, 2016, **6**, 7461–7467.

32 See for example:(*a*) J. E. Poist and C. S. Kraihanzel, *Chem. Commun.*, 1968, 607–608; (*b*) Y. Okuda, Y. Ishiguro, S. Mori, K. Nakajima and Y. Nishihara, *Organometallics*, 2014, **33**, 1878–1889.

33 (*a*) E. G. Robins, X. Liu, N. C. Norman and T. B. Marder, unpublished results; (*b*) E. G. Robins, PhD Thesis, Bristol University, 1997.

34 (*a*) M. Bluhm, A. Maderna, H. Pritzkow, S. Bethke, R. Gleiter and W. Siebert, *Eur. J. Inorg. Chem.*, 1999, 1693–1700; (*b*) For a related tetra-borylation of $(MeO)CH_2$-CC-$CH_2(OMe)$ see:

H. Yoshida, S. Kawashima, Y. Takemoto, K. Okada, J. Ohshita and K. Takaki, *Angew. Chem., Int. Ed.*, 2012, **51**, 235–238.

35 (*a*) N. Cabrera-Lobera, M. T. Quirós, W. W. Brennessel, M. L. Neidig, E. Buñuel and D. J. Cárdenas, *Org. Lett.*, 2019, **21**, 6552–6556; (*b*) N. Cabrera-Lobera, M. T. Quirós, E. Buñuel and D. J. Cárdenas, *Catal. Sci. Technol.*, 2019, **9**, 1021–1029; (*c*) I. Manjón-Mata, M. T. Quirós, E. Velasco-Juárez, E. Buñuel and D. J. Cárdenas, *Adv. Synth. Catal.*, 2022, **364**, 1716–1723.

36 L. Dang, H. Zhao, Z. Lin and T. B. Marder, *Organometallics*, 2008, **27**, 1178–1186.

37 (*a*) L. Kuehn, L. Zapf, L. Werner, M. Stang, S. Würtemberger-Pietsch, I. Krummenacher, H. Braunschweig, E. Lacôte, T. B. Marder and U. Radius, *Chem. Sci.*, 2022, **13**, 8321–8333; (*b*) S. Jos, C. Szwetkowski, C. Slebodnick, R. Ricker, K. L. Chan, W. C. Chan, U. Radius, Z. Lin, T. B. Marder and W. L. Santos, *Chem.–Eur. J.*, 2022, **28**, e202202349.

38 W. Clegg, A. J. Scott, G. Lesley, T. B. Marder and N. C. Norman, *Acta Crystallogr. C*, 1996, **52**, 1991–1995.

39 R. N. Perutz and S. Sabo-Etienne, *Angew. Chem. Int., Ed.*, 2007, **46**, 2578–2592.